AGU PUBLICATIONS

JGR

Journal of Geophysical Research: Atmospheres

RESEARCH ARTICLE
10.1002/2015JD024375

Key Points:
- In-snow processes increase impurity mixing ratios by up to an order of magnitude
- Dust and soil are significant contributors to snow particulate absorption in Utah and Idaho
- Observational/model comparisons need to account for large temporal variations associated with snow aging

Supporting Information:
- Supporting Information S1
- Table S1

Correspondence to:
S. J. Doherty,
sarahd@atmos.washington.edu

Citation:
Doherty, S. J., D. A. Hegg, J. E. Johnson, P. K. Quinn, J. P. Schwarz, C. Dang, and S. G. Warren (2016), Causes of variability in light absorption by particles in snow at sites in Idaho and Utah, *J. Geophys. Res. Atmos.*, *121*, 4751–4768, doi:10.1002/2015JD024375.

Received 20 OCT 2015
Accepted 12 APR 2016
Accepted article online 18 APR 2016
Published online 5 MAY 2016
Corrected 18 MAY 2016

This article was corrected on 18 MAY 2016. See the end of the full text for details.

Causes of variability in light absorption by particles in snow at sites in Idaho and Utah

Sarah J. Doherty[1], Dean A. Hegg[2], James E. Johnson[1], Patricia K. Quinn[3], Joshua P. Schwarz[4], Cheng Dang[2], and Stephen G. Warren[2]

[1]Joint Institute for the Study of the Atmosphere and Ocean, University of Washington, Seattle, Washington, USA, [2]Department of Atmospheric Sciences, University of Washington, Seattle, Washington, USA, [3]Pacific Marine Environmental Laboratory, National Oceanic and Atmospheric Administration, Seattle, Washington, USA, [4]Chemical Sciences Division, Earth System Research Laboratory, National Oceanic and Atmospheric Administration, Boulder, Colorado, USA

Abstract A characterization of black carbon (BC) and other light-absorbing particles in snow is presented for three mountain valley sites in Idaho in early 2014 and for one site near Vernal, Utah, in early 2013 and 2014. The focus of the study was on constraining the magnitude and drivers of variations in particulate absorbers in midlatitude U.S. seasonal snow. Mass mixing ratios of BC in newly fallen snow were similar at all three Idaho sites, with a median of 4.7 ± 4.2 ng BC per gram of snow. The median total light-absorbing particulate mixing ratios in new snow, expressed as an equivalent mixing ratio of BC, was 18 ± 23 ng g^{-1}. At the Utah site, which is near sources of both fossil fuel and dust, the mixing ratios of BC varied from 7 to 45 ng g^{-1} across seven new snowfall samples, and the BC-equivalent mixing ratios varied from 9 to 1500 ng g^{-1}. At all sites, dry deposition and in-snow processes increase the mixing ratio of BC by up to an order of magnitude and increase the mixing ratio of all light-absorbing particulates by up to 2 orders of magnitude, highlighting the importance of capturing these processes for accurately representing snow albedo in climate models. Spatial variability at a range of scales is found to be considerably smaller than the temporal variations at a given site, with implications for the representativeness of field samples used in observation/model comparisons.

1. Introduction

The work presented here builds on our previous regional-scale studies of the amount and sources of black carbon (BC) and other light-absorbing particles in snow in the Arctic [*Doherty et al.*, 2010; *Hegg et al.*, 2009; *Hegg et al.*, 2010], northern China [*Wang et al.*, 2013; *Zhang et al.*, 2013], and midlatitude North America [*Doherty et al.*, 2014]. Each of those studies included vertical profiles at tens of sampling sites spanning hundreds to thousands of kilometers, with each site sampled on an individual day in winter or spring. Except for Greenland and the Arctic Ocean, samples were collected from cold snow that had not yet warmed sufficiently to melt and that very likely had not been rained on (except perhaps for samples from the very bottommost layers, corresponding to early in the snow accumulation season). In addition, we have studied the effect of melt on snow particulate mass mixing ratios at three Arctic sites: the percolation zone of Greenland (Dye-2), on the sea ice near Barrow, Alaska, and on hillsides above Tromsø, Norway [*Doherty et al.*, 2010]. At all three of these Arctic sites combustion aerosol from fossil fuel burning and biomass burning dominated snow particulate absorption [*Hegg et al.*, 2009, 2010]. However, at the midlatitude sites in north China and North America dust often played a significant or dominant role in snow albedo reduction by particles [*Wang et al.*, 2013; *Doherty et al.*, 2014].

Here rather than conducting geographically broad surveys, we study the evolution of the mass mixing ratios and sources of light-absorbing particles in snow in two midlatitude regions in western North America from late winter through spring, when climate forcing via snow albedo reduction is maximized. We compare the evolution in snowpacks expected to be mostly influenced by combustion aerosol (two mountain sites in Idaho), to that in snowpacks expected to be influenced by a mix of combustion aerosol and dust (one northern Utah site and a site in the southern mountains of Idaho, closer to the dry plains in the southern/southwestern part of the state).

We studied seasonal variations specifically at midlatitude sites because seasonal snow there often goes through rapid cycles of above- and below-freezing temperatures, snowfall, and rainfall. A goal was to quantify how much these meteorological variations, as opposed to variations in particulate mixing ratios in falling snow, contribute to particulate mixing ratios in snow on the ground as it ages.

2. Methods

Sample collection and analysis is identical to that described by *Doherty et al*. [2014], hereafter referred to as D14, for a broader survey of North American sites. Whereas D14 reported results for a single vertical profile at each of 67 sites in early 2013, in the present study we collected vertical profiles every few days at each of the three rural sites in central Idaho over approximately two months in early 2014 (Figures S1 and S2). We also collected surface samples, and some vertical profiles, daily at a single site in Utah for about a month each in early 2013 and early 2014. (Figures S1 and S3).

Collection dates at the three Idaho sites varied but spanned 27 January to 24 March 2014. On some days, especially near the beginning of the campaign, only newly fallen snow was collected, but on most sampling days samples were collected at vertical intervals through most or all of the snow depth. The two southern sites (Cascade Valley and Garden Valley) were usually sampled on the same day. At all three sites hard ice layers or water saturation sometimes prevented collection of useful samples from the layer closest to the ground, especially later in the campaign when the snowpack was going through daily melt/freeze cycles.

The Utah samples were collected as part of a larger study (UBWOS or the Uintah Basin Wintertime Ozone Study; *Ahmadov et al*. [2015]) of snow photochemistry and tropospheric ozone in a region influenced by emissions from oil and natural gas extraction. Interest in light absorption by particles in the snow was motivated by trying to quantify actinic flux in the surface snow layer, so snow samples were generally collected of the surface layer only. Samples were collected on a daily basis 28 January to 21 February 2013 and again 17 January to 13 February 2014 (Table S1).

2.1. Sampling Sites and Protocol

Each of the three Idaho sites is in a mountain valley, falling roughly along a north-south line (Figure S2). The McCall site is the northern most and at the highest altitude; 60 km south of this is the Cascade Valley site and a further 35 km south the Garden Valley site. Initial sampling at the McCall site was on Payette Lake (McCall-A), but with rainfall and melt we were forced to move to a nearby peninsula (McCall-B then McCall-C). All three of the McCall subsites are within a 1 km radius. The Cascade Valley and Garden Valley sites were both on farmland. The Vernal, Utah site is located in the Uintah basin, on one of many natural gas and petroleum extraction well pads. More detailed site descriptions are provided in the supporting information.

The sampling protocol followed that of D14. At all sites in Idaho sample layers were selected based on snow morphology. In particular, newly fallen snow was isolated from older snow and crust layers were isolated, so we could study the effects of melt and refreezing (presumably the processes leading to crust formation) on snow particulates.

For each Idaho site we gathered two side-by-side profiles (separated by <1 m) on each sampling day. Impurity data reported here for each "sample" are in fact averages of two side-by-side samples. An exception is the data reported for the McCall-A site on 27 January: On this day, we collected six randomly distributed profiles separated by 10 m; results are averages across all six profiles.

For the Vernal site the sampling was less systematic. When sampling the surface snow only, four to six samples were usually collected. The values shown here are averages across all samples from a given location, date, and depth. In 2013, pairs of samples were usually collected at each depth when sampling a vertical profile. These pairs of samples were averaged. In 2014, usually a single sample was collected at each depth when sampling a vertical profile.

All snow samples were kept frozen until they were intentionally melted in a microwave oven in clean glass jars. The melted snow water was filtered through Nuclepore filters of pore size 0.4 μm, which were then dried and stored in petri dishes for optical analysis. For a subset of the Idaho samples we decanted aliquots of melted snow into 100 mL polyethylene bottles immediately after microwaving, added three drops of chloroform to prevent biological growth, and refroze them. These samples were chemically analyzed in the lab for standard ions, carbohydrates, and various elements, as described in D14, and used in a Positive Matrix Factorization (PMF) analysis. The samples included in the chemical and PMF analyses are indicated in Table S1.

For a second subset of the samples a portion of the collected snow was analyzed for BC not only by our optical method (ISSW) but also by an incandescence technique (the Single Particle Soot Photometer, SP2). All samples included in the ISSW/SP2 comparison were collected at the McCall site, from three depths in the

new snowpack on 10 February, from the surface on 14 February, at three depths on 22 February, and at two depths each on 1 March and 11 March. For this comparison we selected samples only from the McCall site so as to avoid snow heavily laden with dust or soil. All snow samples analyzed with the SP2 were collected in glass jars and kept frozen from the time of sampling until they were intentionally melted in the lab for analysis. As the melt/freeze process appears to cause BC in snow and ice to shift to larger sizes, this procedure ensured undegraded samples to optimize the value of the SP2 measurement [*Schwarz et al*., 2013].

2.2. ISSW and SP2 Analyses

Sample filters were optically analyzed for spectrally resolved absorption using an Integrating Sphere Integrating Sandwich Spectrophotometer (ISSW) [*Grenfell et al*., 2011] that had been modified as described by D14. For each sampled layer we calculated the following quantities based on the ISSW measurements:

C_{BC}^{equiv} (ng g^{-1}) The mixing ratio of BC that would be needed to produce the absorption of solar energy, integrated across 300–750 nm, by all insoluble particles in snow.
C_{BC}^{est} (ng g^{-1}) The estimated mass mixing ratio of BC in snow.
$Å_{tot}$ The absorption Ångström exponent of all insoluble particles in snow, calculated as a linear fit to the logarithm of spectral absorption versus the logarithm of wavelength, 450–600 nm.
f_{nonBC}^{est} The estimated fraction of solar energy absorption across wavelengths 300–750 nm due to insoluble, non-BC components of the particles in snow.

Our measured quantity is absorption, so the mass mixing ratios C_{BC}^{equiv} and C_{BC}^{est} reflect the mass of BC (specifically, the artificial soot fullerene) that would be needed to account for the spectral absorption by all particles (C_{BC}^{equiv}) and by BC only (C_{BC}^{est}). We estimate the mass absorption efficiency of fullerene as 8.9, 7.2, and 6.5 m^2 g^{-1} at 450, 550, and 600 nm, respectively [D14]. The product of C_{BC}^{equiv} and f_{nonBC}^{est} is a metric for the light absorption by non-BC particulates, also expressed as a BC mass mixing ratio; this product was input to the PMF analysis as "non-BC absorption." For a full description of how these quantities are derived, see supporting information [*Grenfell et al*., 2011; *Doherty et al*., 2010].

Absorption is attributed to BC and non-BC components using assumed values of the absorption Ångström exponent for these components and by assuming that $Å_{tot}$ results from a linear combination of these components' contributions to absorption (see supporting information for more details). *Doherty et al*. [2010] assessed the measurement uncertainty in C_{BC}^{est} caused by uncertainties in the values of *Å* used for attribution to the BC and non-BC components (see their Figure 16 and associated discussion), as well as other ISSW uncertainties. *Schwarz et al*. [2012] subsequently showed that the ISSW estimate of BC mixing ratios, C_{BC}^{est}, in liquid samples was biased high by about 40% for a set of lab-generated liquid samples containing water and a BC reference material (fullerene soot) only [*Schwarz et al*., 2012, Figure 3]. In that analysis the BC mixing ratios were gravimetrically determined (BC_{grav}). They also found that for liquid samples containing a mix of fullerene soot and dust the ISSW bias in C_{BC}^{est} increased with increased dust concentration, up to a factor of 3. In the same study, the SP2 estimate of BC mixing ratios (rBC) was found to have a small (5%) low bias for the BC-only samples, with very little sensitivity to dust.

To test whether similar differences were found in field samples, a subset of the newly fallen snow samples from the McCall-A site were analyzed with both the ISSW and an SP2 (see supporting information), and the estimates of BC mixing ratios compared. The results of this comparison are given in section 3.1 below. Based on the combined results of this analysis and the *Schwarz et al*. [2012] study, all C_{BC}^{est} values reported herein have been adjusted. The adjustment factor is based on a linear fit to the ratios of C_{BC}^{est} to BC_{grav} (for samples from the *Schwarz et al*. [2012] study) and C_{BC}^{est} to BC_{SP2} (for SP2-analyzed field samples reported herein) versus ISSW filter loading (thick gray line in Figure 1b)). Using this adjustment, values of C_{BC}^{est} were scaled down, with the correction factor depending on each sample's filter loading; these adjusted values are hereafter referred to as $C_{BC}^{est'}$. For the data presented herein, C_{BC}^{est} was scaled down by, on average, 2.5 ± 0.9. In making this adjustment we are assuming that there is no low bias in rBC for the 2014 Idaho snow samples. If there is, the values of $C_{BC}^{est'}$ presented here may in turn be biased low.

Note that C_{BC}^{est} values from earlier studies using the ISSW [i.e., *Doherty et al*., 2010, 2013, 2014; *Wang et al*., 2013] did not apply this correction. Accordingly, comparisons of $C_{BC}^{est'}$ presented here to C_{BC}^{est} in those studies

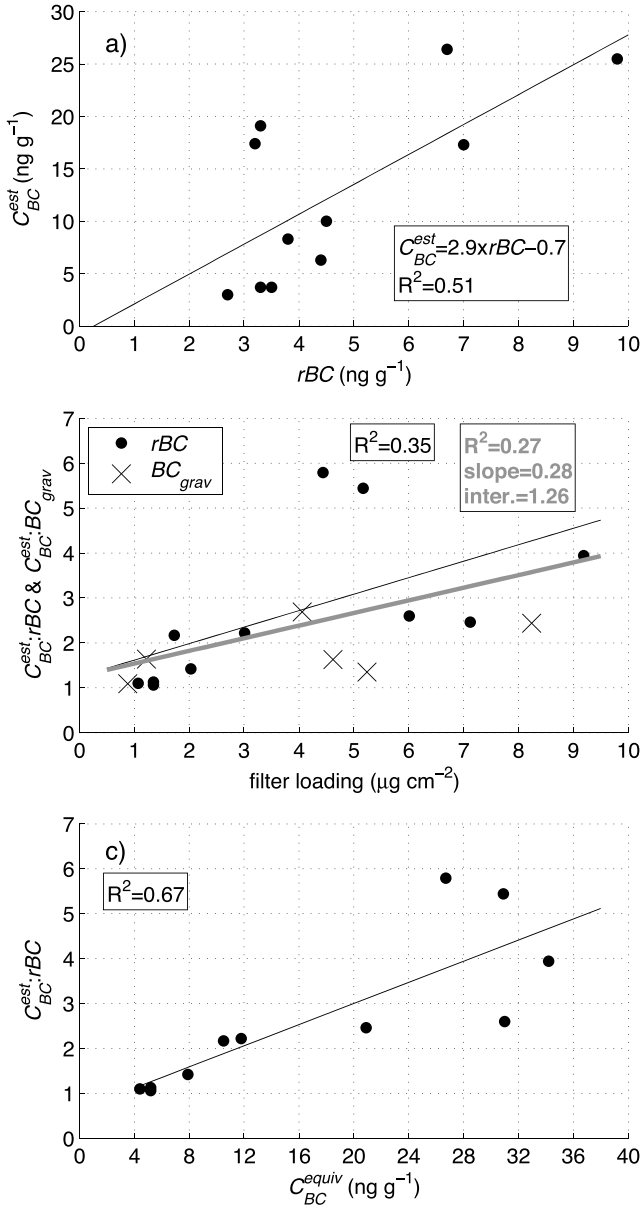

Figure 1. (a) Estimates of the mass mixing ratio of BC in snow from the ISSW (C_{BC}^{est}) compared to those from the SP2 (rBC) for a subset of 11 newly fallen snow samples from the McCall, Idaho site. (b) The ratios C_{BC}^{est}:rBC and C_{BC}^{est}:BC_{grav} as a function of filter loading in the ISSW analysis. (c) The ratio C_{BC}^{est}:rBC as a function of C_{BC}^{equiv} from the ISSW analysis. The comparison to BC_{grav} in Figure 1b is for all samples containing a mix of the synthetic BC fullerene and a dust standard, included in *Schwarz et al.* [2012]. The two fit lines and values of R^2 in Figure 1b are for the 2014 Idaho samples only (black line and text) and for the combined Idaho and fullerene/dust standard samples (thick gray line and bold gray text).

should be conducted with this in mind (Note that both corrected and uncorrected data are available at http://www.atmos.washington.edu/articles/IdahoUtah2014). Further, there is between 10% (low filter loading) and 60% (high loading) uncertainty added to $C_{BC}^{est'}$ due to uncertainty in the correction factor. Despite the resulting elevated uncertainty, we think that the repeat finding of apparent high biases in C_{BC}^{est} from the ISSW merited making this correction.

2.3. Chemical and PMF Analysis

Snow water samples saved for chemical analysis were analyzed for a suite of species to aid in source attribution via PMF analysis. The analytes, and the techniques used to quantify them, are as follows: Levoglucosan, glucose, and mannitol concentrations were derived from liquid chromatography-mass spectrometry (LC-MS). Formate, chloride, nitrate, succinate, sulfate, and oxalate were derived from standard ion chromatography. Sodium, aluminum, silicon, potassium, calcium, titanium, vanadium, chromium, manganese, magnesium, iron, nickel, copper, zinc, arsenic, selenium, and lead were quantified with inductively coupled mass spectrometry (ICP-MS). Vanadium, lead, arsenic, and selenium had very poor signal-to-noise ratios for this data set, with too many zero values, and therefore could not be employed in any of the analyses. Mixing ratios of the chemical components and the values of C_{BC}^{equiv} and $C_{BC}^{est'}$ from the optical analysis were input to a Positive Matrix Factorization (PMF) analysis to determine the sources of total particulate absorption.

The PMF analysis groups into orthogonal "factors" those constituents in the snow that covary, implying that they share a common source. The chemical composition of each factor is interpreted for what source type it best represents, taking into account likely emission sources in the region of interest. Details of the chemical and PMF analyses can be found in D14. The only difference from D14 is that here we did not separately analyze for absorption by organic carbon (OC_{abs} in D14), and here we input to the PMF C_{BC}^{equiv} rather than C_{BC}^{max}. Chemical and PMF analyses were not conducted for the Utah samples. More details of the PMF analyses can be found in supporting information.

2.4. Meteorological Records

Daily weather logs were kept during the Idaho field campaign, manually recording surface air temperatures and periods of precipitation. In addition, we downloaded data from monitors at two nearby SNOTEL (Snow Telemetry; http://www.wcc.nrcs.usda.gov/snow/) sites. The Secesh summit SNOTEL site (45.1833°N, 115.9667°W, 1987 m altitude) is in the mountains 25 km north and 11 km east of the McCall site, and the Long Valley SNOTEL site (44.7833°N, 116.0833°W, 1490 m altitude) is 18 km south of the McCall site and 40 km north of the Cascade Valley site, in the broad north-south valley between the two (Figure S2). The Long Valley SNOTEL reports are likely more indicative of conditions at our two northern sampling sites, and the Secesh summit winds are likely a better indicator of air mass source region at cloud altitudes.

An automated weather station at the Utah site logged air temperature and wind data at one-minute resolution at multiple levels 2–18 m above the surface in both 2013 and 2014. From these we compute daily averages, minima, and maxima of these parameters.

3. Results and Discussion

3.1. ISSW/SP2 Comparison

Figure 1 compares the estimated mixing ratios of BC in snow from the ISSW (C_{BC}^{est}; i.e., the uncorrected values) to those from the SP2 (rBC) for 11 newly fallen snow samples from McCall, Idaho (section 2.1). Estimates of BC mixing ratio from the ISSW are, on average, almost a factor of three higher than those from the SP2. In addition, the two are only moderately correlated ($R^2 = 0.5$). As discussed in section 2.2, tests with a BC standard (fullerene soot) and a dust standard showed that the ISSW has high biases in C_{BC}^{est} when BC is mixed with dust and that the bias increases with the amount of added dust [*Schwarz et al*., 2012]. Since dust (and essentially all other absorbing aerosol) has a higher absorption Ångström exponent than BC, based on the results of *Schwarz et al*. [2012], we would expect that the ratio C_{BC}^{est}:rBC (i.e., the high bias in C_{BC}^{est}) would increase with $\mathring{A}_{tot}$—i.e., as the amount of dust or other non-BC components in the sample increases. However, for this set of 11 field samples, across which $\mathring{A}_{tot}$ varies from 1.5 to 2.4, there is very poor correlation between C_{BC}^{est}:rBC and $\mathring{A}_{tot}$ ($R^2 = 0.16$; not shown in Figure 1).

The ratio C_{BC}^{est}:rBC is better correlated with filter loading ($R^2 = 0.35$), suggesting an artifact from the optical effects of a mix of scattering and absorbing particles on a filter (wherein multiple scattering enhances absorption; e.g., *Bond et al*. [1999] and *Lack et al*. [2008]). This is also consistent with the finding of *Schwarz et al*. [2012] that the ISSW demonstrated sensitivity to a purely scattering aerosol. The ratio is even better correlated with C_{BC}^{equiv} ($R^2 = 0.67$). C_{BC}^{equiv} and filter loading are themselves correlated ($R^2 = 0.80$; not shown), simply because we tended to filter similar amounts of snow water for all 11 samples. Thus, it is not possible to determine whether the differences in the ISSW and SP-2 are physically linked to snow particulate mixing ratios or to effects of filter loading.

Given the correlations shown in Figure 1 for the field samples, we reanalyzed the samples of *Schwarz et al*. [2012] with mixes of a dust standard and fullerene soot using the current version of the ISSW. As for the field samples, the correlation of the ratio C_{BC}^{est}:BC_{grav} with C_{BC}^{equiv} ($R^2 = 0.57$) is higher than it is with filter loading ($R^2 = 0.31$). The additional correlation between the bias in C_{BC}^{est} and the amount of dust in the samples noted by *Schwarz et al*. [2012] may result from the fact that filter loading and C_{BC}^{equiv} are themselves correlated with the amount of dust added to the test sample.

As noted above, we used the fit for the combined data set from Idaho 2014 and *Schwarz et al*. [2012] (slope = 0.28, *y* intercept = 1.26; see thick gray line in Figure 1b) to adjust C_{BC}^{est} for all the field samples presented herein, yielding corrected values $C_{BC}^{est'}$. For the field samples it is possible that biases in the SP2 contribute to the ratio C_{BC}^{est}:rBC, in which case we may be overcorrecting C_{BC}^{est}. As discussed by *Schwarz et al*. [2012], accurate estimates of rBC rely in part on efficiently transmitting particles in the liquid sample to the instrument via a nebulization system. It is unlikely that BC attached to very large particles (e.g., $>10\,\mu m$) will reach the SP2 sample chamber. For this reason we did not include samples heavily laden with dust in the 2014 field sample comparisons. Thus, it seems unlikely that this process is contributing significantly to the value of the ratio C_{BC}^{est}:rBC, especially given the lack of correlation with $\mathring{A}_{tot}$. However, we emphasize that this

source of potential bias in the SP2 might be important in dust-dominated aged snow and ice, and it is currently unquantified.

3.2. Idaho: Meteorology and Snowpack Evolution:

When we arrived in McCall on 26 January, there was only 8 cm of snow on Payette Lake. The previous appreciable snowfall at the Long Valley SNOTEL site, of approximately 7–8 cm, was on 8–11 January. Thus, by 27 January (our first sampling day) the surface snow had been exposed to an extended window of opportunity for dry deposition as well as sublimation and possibly some surface melting, especially at our two lower elevation sites. At those sites there was 3–4 cm of crust on top of 10 cm (Cascade Valley) and 7 cm (Garden Valley) of large-grained old snow, all of which had clearly been through at least one significant melt-freeze cycle. Based on the temperature data from the Long Valley SNOTEL site, melting at the McCall site was likely limited and restricted to the surface snow.

On 28–29 January the McCall site got 15 cm of new snow on top of the existing 8 cm, and the more southern Idaho sites got 3 cm (Cascade Valley) and a trace ($<$0.5 cm; Garden Valley). For the remainder of the first two weeks of February snow accumulated at all three sites. Then a warm, wet event brought rainfall and afternoon temperatures that rose above freezing. This melt/rain event forced us to move our sampling from the McCall-A site to the McCall-B site (first vertical black line in Figure 2). During the second half of the month there were frequent diurnal melt/freeze cycles, especially at the two more southern sites. Precipitation alternated between snow and a rain/snow mix. At the Cascade Valley and Garden Valley sites, nearly the entire snowpack melted over a few days with rapid warming on 25–28 February (day of year, DOY, 56–59). These two sites were sampled for the last time on 4 March (DOY 63), when all that remained was 3–6 cm of patchy, icy snow on top of a mix of ice and meltwater (which was not sampled). At the McCall site, nighttime temperatures were below freezing for the first week of March, sometimes with overnight snowfall, but during the day it warmed to above freezing (typically 1–3°C) with light rainfall on many days. On 8 March (DOY 67) it was clear and sunny with a high again around 2°C, but on 9 March it rained heavily, with $>$3 cm of rain falling between sunrise and noon. On 10 March temperatures dropped, and overnight 10–11 March there was 8 cm of new snowfall. Snow fell again on 14 March (DOY 73) (2 cm) and March 17 (DOY 76) (1 cm) but otherwise for 12–24 March (DOY 71–83) days were dry with temperatures dropping to −7°C at night and rising to 1–4°C during the day. The McCall site was last sampled on 24 March.

3.3. Idaho: Evolution of Light-Absorbing Particles in Snow

3.3.1. Snow Particulate Mixing Ratios and Å_{tot}

As noted above, there had been no appreciable new snowfall for more than 2 weeks before field sampling started. This aged surface snow was sampled at McCall-A on 27 January (DOY 27) and was sampled as a subsurface layer below newly fallen snow at the Cascade Valley and Garden Valley sites on 1 February (DOY 32) (Figure 2). New snowfall events in the first half of February lowered particulate mixing ratios. Alternating periods of snow melt, rainfall (pink vertical lines in Figure 2), and new snowfall (sample layers with white dots in the center in Figure 2) from DOY 41 onward were accompanied by large variations in the surface snow mixing ratios of light-absorbing particles at all three sites.

When we transitioned from site McCall-B to McCall-C on 14 March (day 73; second vertical black line in Figure 2) C_{BC}^{equiv} and $C_{BC}^{est'}$ at 0–2 cm depth were nearly identical at the two sites, but at 2–6 cm depth C_{BC}^{equiv} and $C_{BC}^{est'}$ at McCall-C were about twice that at McCall-B. Note that total snowpack depth was greater at McCall-A than McCall-B, largely because snow accumulated at McCall-A only after the lake had frozen. The difference in total snowpack depth from McCall-B to McCall-C (both on land) was less pronounced and is likely due to differences in the effects on accumulation and sublimation of the greater tree cover at McCall-C (wooded) versus McCall-B (open grassland).

Several things are qualitatively apparent from Figure 2: C_{BC}^{equiv} and $C_{BC}^{est'}$ are both lower for newly fallen snow than for aged snow; C_{BC}^{equiv} and $C_{BC}^{est'}$ are more similar in newly fallen snow than in aged snow samples; and late in the sampling period, after there has been significant melting, the surface snow mixing ratios are higher. Less apparent is the effect of rainfall on C_{BC}^{equiv} and $C_{BC}^{est'}$ because rainfall was usually accompanied by temperatures warm enough to independently melt surface snow; thus, it is difficult to disentangle the effects of the two. An exception is one pair of samples gathered in McCall on 3 March (DOY 61). A 1 cm deep layer of newly

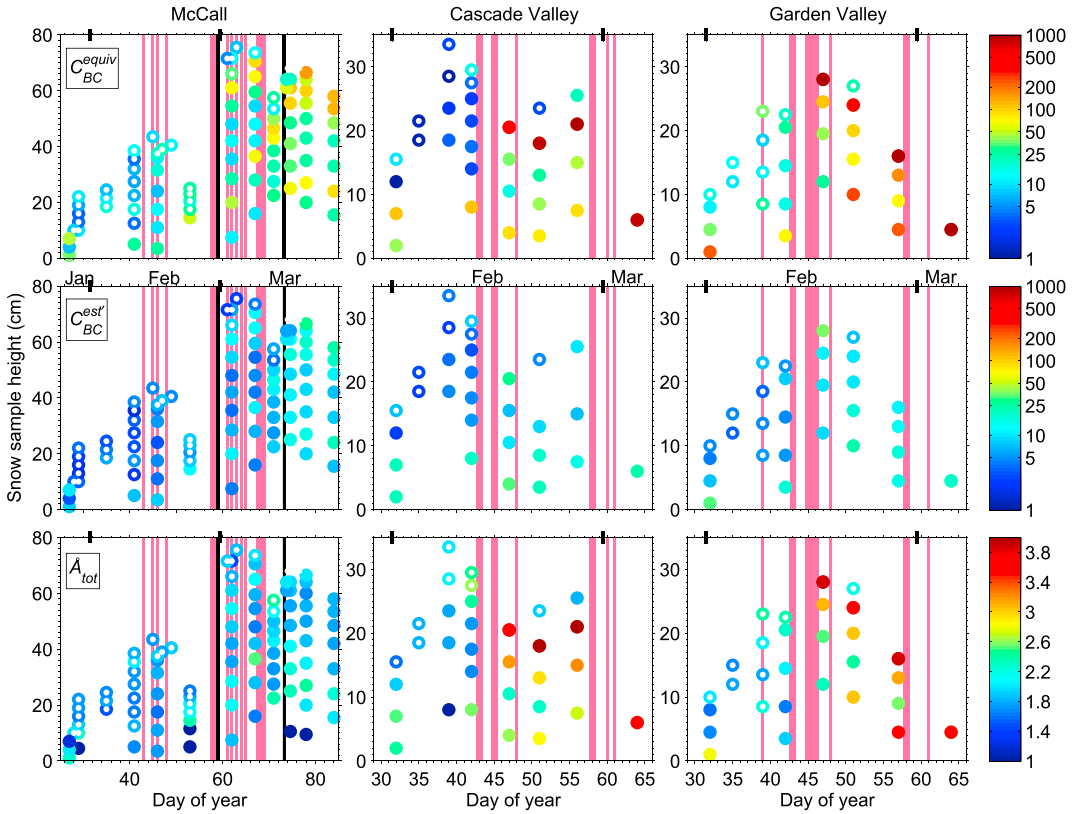

Figure 2. Time series of (top row) C_{BC}^{equiv}, (middle row) $C_{BC}^{est'}$, and (bottom row) $\AA_{tot}$ versus sample height above the surface for the three Idaho sampling sites (first to third columns). Dot color indicates the value, as given in the color bar. Samples that were of new snow (≤1 day old) are marked with a small white dot in the center. Vertical pink lines indicate rain events; thick pink lines indicate heavy rainfall. During the entire period sampled at all three sites temperatures dropped below freezing at night, so days with melt in fact had at least a diurnal melt/freeze cycle. Days with rain may also have had mixed rain and snow. At the McCall site, the switch from McCall-A to McCall-B and then McCall-C is marked with vertical black lines. Late on DOY 73 and early on DOY 76 new snow fell at McCall but was not sampled.

fallen snow was sampled immediately after falling, just as precipitation was transitioning from snow to rain. This same layer was then resampled after being rained on for four hours, with temperatures holding at approximately 0°C. After being rained on, $\AA_{tot}$ was unchanged but $C_{BC}^{est'}$ and C_{BC}^{equiv} increased by about a factor of 2.5 and 3.5, respectively. This rapid increase in surface snow particulate mixing ratios is comparable to the factor of 3–5 enhancement in surface snow particulate mixing ratios observed by *Doherty et al*. [2013] in rain-free melting snowpacks. The fact that $\AA_{tot}$ was unchanged suggests that the rain did not preferentially remove specific particulate components, e.g., brown organics versus black carbon. What is unclear is whether the higher mixing ratios can be attributed to preferential removal of snow water over snow particulates or to elevated mixing ratios of particulates in the rain water itself, which now saturated the recently fallen snow.

We expected that new snowfall would be cleaner to the north, deeper in the mountains, and farther away from the city of Boise. However, $C_{BC}^{est'}$ and C_{BC}^{equiv} for newly fallen snow were similar at all three sites (Table 1). In contrast, $C_{BC}^{est'}$ for aged snow samples increases modestly from north to south, and C_{BC}^{equiv} increases significantly north to south. Means and medians differ much more in the aged samples than in new snow, and the mixing ratios and $\AA_{tot}$ are higher and more variable in the aged snow samples. This contrast shows that processes following wet deposition strongly determine both spatial and temporal variations in snow particulate light absorption.

Ideally, we would have a record of the age, temperature, melt rate, and sublimation rate for all sampled snow layers, as well as rainfall rate, amount of rain water retained in the snowpack, and C_{BC}^{equiv} and $C_{BC}^{est'}$ in the rainwater,

Table 1. Mixing Ratios C_{BC}^{equiv} and $C_{BC}^{est'}$ and the Absorption Ångström Exponent, $Å_{tot}$, Across All *n* New Snow or Aged Snow Samples at Each of the Three Idaho Study Sites

	C_{BC}^{equiv} (ng g^{-1})				$C_{BC}^{est'}$ (ng g^{-1})			$Å_{tot}$		
	n	Mean	Median	SD	Mean	Median	SD	Mean	Median	SD
New Snow Samples										
McCall	31	13.3	11.3	8.6	4.6	4.3	2.1	1.85	1.81	0.22
Cascade Valley	9	15.6	11.3	12.9	4.5	4.2	2.2	2.03	1.97	0.34
Garden Valley	8	18.3	15.5	9.0	5.1	4.9	1.3	2.06	2.04	0.27
Aged Snow Samples										
McCall	66	42.1	28.9	33.5	9.8	8.5	5.4	1.77	1.84	0.56
Cascade Valley	28	218.2	92.0	278.7	13.3	10.1	9.5	2.66	2.60	0.95
Garden Valley	26	405.5	138.8	649.8	14.9	11.8	8.9	2.66	2.93	1.08

so we could study how each affects profiles of snow mixing ratios and $Å_{tot}$. Lacking this, we use snow density, ρ, as a first-order proxy for effective snow age, where "effective age" relates both to the time elapsed since the snow fell—i.e., exposure to dry deposition and sublimation—and to exposure of the snow to warm temperatures and rainfall.

Note that increasing snow density via compaction does not affect particulate mixing ratios nor, by itself, does a change in snow grain size, since neither of these processes affects the ratio of snow particle mass to snow water mass. Processes that do affect the mixing ratios of particles in snow are the addition of particles to snow via dry deposition or mechanical mixing (e.g., of local soil into the snowpack), loss of snow water via sublimation, addition of snow water by frost deposition at the snow surface, loss of snow water via melting, and loss of particles through wash out with snow meltwater or rainfall. Melting followed by refreezing of the meltwater within the snowpack and depth hoar formation will redistribute particles within the snow column but cannot change the total particulate mass in the snow column.

As a further indicator of snow age and degree of postdeposition processing we classify each sample as newly fallen snow, pack snow, or crust, with allocation to the latter two categories based on observed snow morphology in the sample layer. Here we use "pack snow" generically to include all snow types (e.g., compacted snow, granular snow, and depth hoar) other than newly fallen snow or crust. "New snow" was almost always sampled 12 h or less after it fell. Exceptions are the "new snow" samples at all three Idaho sites on 4 Feb (DOY 35), collected $<$36 hrs after falling, and those from McCall-A on 10 Feb (DOY 41), collected $<$48 hrs after falling. In Figure 3, we plot C_{BC}^{equiv}, $C_{BC}^{est'}$, and $Å_{tot}$ as a function of snow density, segregating the data by site (Figures 3a, 3c, and 3e) and snow type (Figures 3b, 3d, and 3f).

The snow particulate mixing ratios increase approximately exponentially with density at all three sites (Figures 3a and 3c). In McCall, the increase in the mixing ratio of all light-absorbing particles (C_{BC}^{equiv}; Figure 3a) is similar to that for BC only ($C_{BC}^{est'}$). However, at the Cascade and Garden Valley sites, for $\rho > 250$ kg m^{-3} C_{BC}^{equiv} rises more dramatically with density than does C_{BC}^{est}. These elevated values of C_{BC}^{equiv} correspond directly to higher values of $Å_{tot}$ (Figures 3e and 4).

For $\rho < 250$ kg m^{-3} $Å_{tot}$ is variable but has no dependence on snow density or snow type (Figures 3e and 3f). In this density range $Å_{tot}$ is always less than 2.7. However, for many of the more aged/higher density snow samples $Å_{tot}$ is in the range 2.8–4.3. In these samples a particulate component with higher absorption Ångström exponent (i.e., a browner component) has apparently been added to the snow or the blacker components removed. With the latter process C_{BC}^{equiv} is expected to decrease with $Å_{tot}$, and instead, it increases, consistent with the addition of absorbing particles (Figure 4).

Classifying the data by snow type, we see that variations in $C_{BC}^{est'}$ and C_{BC}^{equiv} do not correlate with snow density (Figures 3b and 3d) or with $Å_{tot}$ (Figure 4b) in new snow, but both $C_{BC}^{est'}$ and C_{BC}^{est} increase systematically with density (i.e., age) in the snowpack. New snow can have a range of densities depending on temperature and wind speed at the time the snow fell (i.e., by packing the newly fallen snow) [*Judson and Doesken*, 2000], but these processes do not affect snow particulate mixing ratios. In the snowpack, C_{BC}^{equiv} also increases exponentially with both density (Figure 3) and $Å_{tot}$, for $Å_{tot} > 2.0$ (Figure 4). For $Å_{tot} < 2.0$, variations in C_{BC}^{equiv} are poorly correlated with $Å_{tot}$ for all snow types.

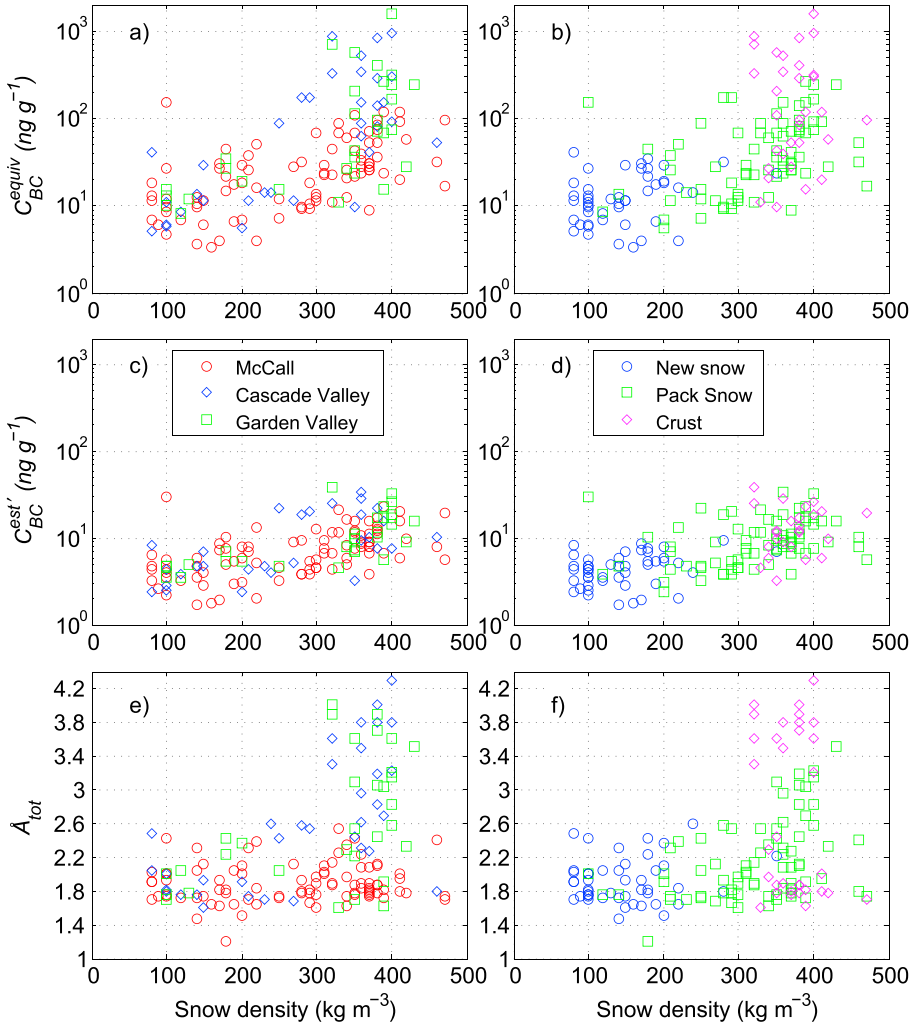

Figure 3. (a and b) C_{BC}^{equiv}, (c and d) $C_{BC}^{est'}$, and (e and f) $Å_{tot}$ versus snow density for all sample layers from the Idaho 2014 study, grouped by (Figures 3a, 3c, and 3e) sampling site and (Figures 3b, 3d, and 3f) snow type. Note the logarithmic scale in Figures 3a–3d.

$C_{BC}^{est'}$ and C_{BC}^{equiv} vary by approximately 1 and 2 orders of magnitude, respectively, across different crust samples (Figures 3b and 3d), but this variation shows no dependence on crust density. Rather, mixing ratios in crust are associated with changes in $Å_{tot}$ (Figure 4), a proxy for particulate composition. The highest mixing ratios of total particulate light absorption (i.e., $C_{BC}^{equiv} > 300$) are for crust samples with $Å_{tot} > 3.2$; all of these samples are from the two southern sites (Cascade Valley and Garden Valley). In crust samples with lower mixing ratios ($C_{BC}^{equiv} < 200$) $Å_{tot}$ is between 1.45 and 2.60, approximately the same range of $Å_{tot}$ found in our newly fallen snow samples (Figures 3f and 4). This group of data includes crust samples from all three sites.

Collectively, these data show that snow is cleanest when it is first deposited to the surface and grows dirtier as it is exposed to the combined effects of dry deposition and in-snow processes. This is not surprising given that dry deposition, sublimation, and melt all increase the ratio of light-absorbing particulate to snow mass. The strong enhancement of snow particulate mixing ratios in the snow surface layer with melting in particular has been demonstrated in field measurements [e.g., *Conway et al.*, 1996; *Xu et al.*, 2012; *Doherty et al.*, 2013], but other processes have been less emphasized.

Our data are not sufficient to quantitatively distinguish the effects of sublimation, melt, rainfall, and dry deposition on snow particulate mixing ratios. However, we can approximately infer the relative roles of

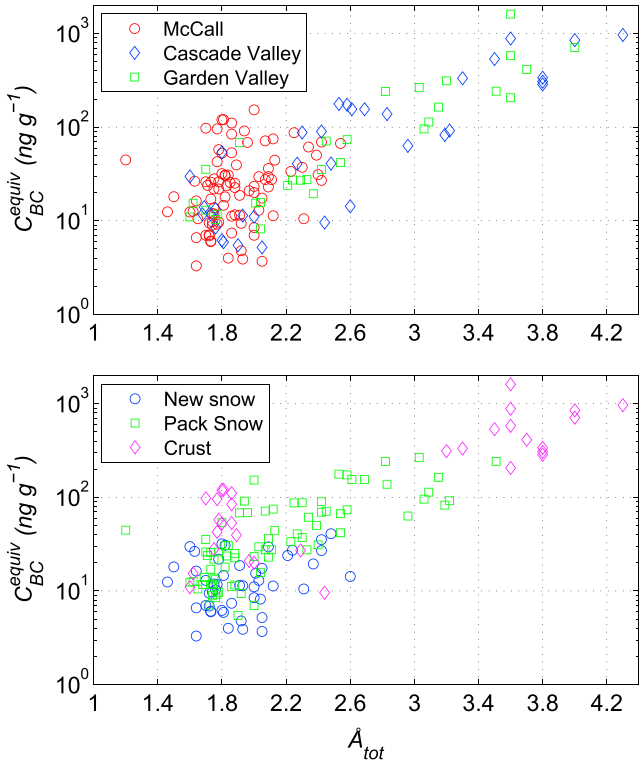

Figure 4. C_{BC}^{equiv} versus $Å_{tot}$ for all sample layers from the Idaho 2014 study, grouped by (top) sampling site and (bottom) snow type.

different processes from combined examination of Figure 4 and the sources of light-absorbing particles in new versus aged snow. The latter is given in Figure 5, which shows the results of the PMF analysis.

3.3.2. Source Attribution of Particulate Absorption

In order to evaluate potentially differing sources for light-absorbing particles in old and new snow, independent PMF analyses were run for three groupings of the samples for which we have chemical data (section 2.4): all samples, old (aged) snow only and newly fallen snow only. For the "all" and "old snow" sample sets the best PMF solution yielded five factors whose chemical fingerprints we identified as associated with Waste incineration, Secondary reactions (i.e. aerosols formed in the atmosphere from gaseous precursors), soil, fossil fuel combustion (FF), and a combination of a strong biomass burning (BB) signature and elements associated with Soil (Figures 5a and 5c). For the "new snow" samples, the PMF yielded four factors. These had chemical fingerprints that overlapped with but were not identical to those from the "all" and "old" snow groupings: Waste, Secondary, Soil, and a mix of biomass and fossil fuel burning (BB + FF) (Figure 5b).

The factor containing the signatures of both fossil fuel burning and biomass burning (FF + BB) and the factor containing both biomass burning and soil (BB + Soil) can be explained by the scavenging of aerosol from air masses where emissions from separate sources are well mixed, leading to a chemical fingerprint that does not distinguish the two. The three leftmost columns in the Figure 5 panels (C_{BC}^{equiv}, $C_{BC}^{est\prime}$, and non-BC absorption) show that while the FF, BB, Soil, and Secondary factors all contribute to particulate light absorption the contribution by the Waste Incineration factor was negligible.

The attribution of particulate absorption in the snow to a "Secondary" aerosol source seems nonphysical, since BC can only form as a primary product of combustion. This can be explained by two things: First, secondary organics resulting from products emitted along with BC from combustion sources can absorb light [e.g., *Washenfelder et al.*, 2015, and references therein], contributing to C_{BC}^{equiv}. Second, particles in the snow may have been scavenged from a well-mixed, aged air mass, such that BC and other light-absorbing primary particles are *associated with* the chemical products of heterogeneous secondary production while not being a product of these reactions. Clearly, the original source of BC must be combustion, but the air mass containing this BC could be sufficiently aged and processed that the dominant chemical fingerprint is of secondary reaction products (e.g., oxalate).

Across the entire data set ("all snow," Figure 5a) variations in BC ($C_{BC}^{est\prime}$) are driven about equally by the Secondary, FF, and BB + Soil factors. However, for total particulate absorption the Secondary factor dominates, accounting for 78 ± 12% of the variance in C_{BC}^{equiv}; the FF factor contributes most of the remaining variance (16 ± 2%). This high association of C_{BC}^{equiv} with the Secondary factor is consistent with the snow particulates including both primary combustion particles (BC and "brown" carbon) and secondary aerosol, some of which may be light absorbing.

The "all snow" PMF analysis is the most robust of the three because it contains the largest number of samples ($n = 68$). However, it does not allow us to distinguish the relative roles of wet deposition and post wet deposition

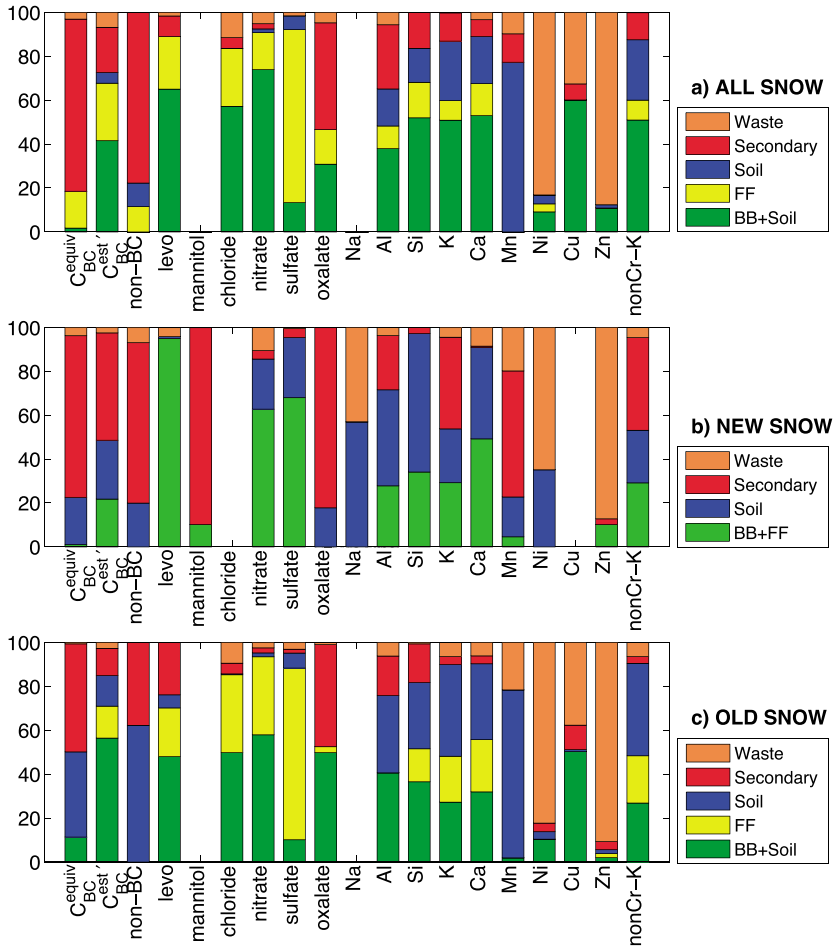

Figure 5. Factor fingerprints for (a) all snow samples, (b) newly fallen snow samples only, and (c) old snow samples only. The leftmost two columns show the sources associated with variations in total particulate absorption (C_{BC}^{equiv}) and absorption by BC only ($C_{BC}^{est'}$). All other columns show the fraction of variation in various chemical components associated with source factors—i.e., the factor chemical "fingerprint" used to identify the source type. ("Waste" = waste incineration; "Secondary" = secondary aerosol production; "FF" = fossil fuel combustion; "BB" = biomass burning combustion). The variable non-BC is the non-BC absorption, calculated as the product of f_{nonBC}^{est} and C_{BC}^{equiv}; "levo" is levoglucosan; and non-Cr-K is non-crustal potassium.

processes in determining variations of C_{BC}^{equiv} and $C_{BC}^{est'}$. Thus, we turn to the PMF analyses of new snow samples only ($n = 35$) and old snow samples only ($n = 33$), keeping in mind that these analyses are less certain because of the reduced number of samples available and the consequent reduction in constraints for the variance analysis.

In newly fallen snow (Figure 5b) most of variability in total particulate absorption (C_{BC}^{equiv}) is associated with the Secondary source (74 ± 11%), with contributions from Soil (22 ± 4%) accounting most of the remaining variation. Variability in non-BC absorption is also mostly driven by the Secondary Factor (78 ± 12%), with the remaining 20% driven equally by the Soil and BB + FF factors. Variations in BC ($C_{BC}^{est'}$), however, are less strongly driven by the Secondary factor (49 ± 9%), with the Soil and BB + FF factors now contributing 27 ± 3% and 21 ± 3%, respectively. The attribution of variability in BC to the Soil factor could be the result of an air mass containing BC (i.e., emitted by a combustion source) having a dominant chemical fingerprint of soil or by there actually being BC mixed in the soil, resuspended with the soil, and deposited to the snowpack.

With snow aging, the contribution by the Secondary factor to total particulate light absorption (C_{BC}^{equiv}) decreases from 74 ± 11% (Figure 5b) to 50 ± 9% (Figure 5c), and an increased fraction of the variability comes from the combined soil and BB sources (50 ± 4% together). For BC, the Secondary factor is even less significant in aged snow (12 ± 3%), with the combined Soil plus BB + Soil (70 ± 5%) and FF (15 ± 3%) factors driving most of the variability.

These changes in the sources of BC to the snow are consistent with (a) dry-deposited aerosols being added to the snowpack; (b) the dry-deposited aerosol coming from a less aged air mass (i.e., clearer FF and BB chemical fingerprints) than the wet-deposited aerosol (which has a more dominant Secondary fingerprint); and (c) significant addition of soil to the snowpack in the days following snowfall events. This makes sense for the mountain valley sites in our study. Wet-scavenged particles generally come from higher up in the atmosphere (e.g., cloud altitudes) than do dry-deposited particles. We observed that at all three sites nighttime inversions often develop, trapping locally emitted smoke (e.g., from wood stoves and slash burning) and pollution (e.g., from trucks) in visibly distinct layers in the mountain valleys. These inversions were more common on clear days/nights, when dry deposition dominates particulate contributions to the snowpack. On days with precipitation, the wind direction at 2000 m altitude typically was from the south/southwest (Figure S4), which is the direction of the city of Boise and associated suburbs and industrial areas. Wind speeds both aloft and in the valley were also higher on days with precipitation (Figure S5), so wet-scavenged aerosol is more likely to have been transported into the area, whereas dry-deposited aerosol may be strongly influenced by fresher, more local sources.

The greater dominance of soil as a source of total particulate absorption in the snow is also consistent with the site locations. The southern two sampling sites are located in mountain valleys with dirt roads and agricultural fields that had patchy snow cover later in the sampling season. In addition, the semiarid hillsides in the region at these two sites may have contributed dust to the valley snow.

3.3.3. Processes Affecting Evolution of Snow Particulate Absorption

Information on the sources of light-absorbing particles in new versus aged snow can be combined with the relationships shown in Figure 4 for insight to which physical processes drive increases in particulate absorption in the aging snowpack. Snow water sublimation and the dry deposition of aerosol that has the same absorption Ångström exponent as wet-deposited aerosol will lead to increases in C_{BC}^{equiv} with no accompanying change in $Å_{tot}$. Snow melt can also increase C_{BC}^{equiv} without changing $Å_{tot}$ as long as snowmelt does not preferentially remove specific particulate components. We conclude that some combination of these three processes account for the observed difference between C_{BC}^{equiv} in aged snow samples versus newly fallen snow samples with the same $Å_{tot}$ (Figure 4). Considering only samples with $1.4 < Å_{tot} < 2.6$, C_{BC}^{equiv} increases by about a factor of 2.5–3 from newly fallen snow (mean 14.6 ng g^{-1}; median 11.7 ng g^{-1}; standard deviation 9.5 ng g^{-1}) to aged snow (mean 43.5 ng g^{-1}; median 28.1 ng g^{-1}; standard deviation 38.1 ng g^{-1}).

Increases in C_{BC}^{equiv} that are accompanied by an increase in $Å_{tot}$, as observed for old snow and crust samples with $Å_{tot} > 2.6$ (Figure 4), are consistent with several processes. First, this could be due to dry deposition to the snowpack of aerosols that have a higher absorption Ångström exponent than wet-deposited aerosols (i.e., those contributed with snowfall). $Å_{tot}$ in newly fallen snow samples is always in the range 1.4–2.6. These are typical values of $Å$ for fossil fuel and biomass burning aerosols [*Doherty et al.*, 2010, and references therein]. $Å$ for local soil samples gathered from the fields at our two southern sites are 3.5–3.7. Dirt on the roads adjacent to the Cascade Valley site has a similar $Å$ (3.7), but in soil from the road adjacent to the Garden Valley site it is even higher: 5.2. The addition (by dry deposition) of soil to the snowpack will therefore simultaneously increase C_{BC}^{equiv} and $Å_{tot}$. Indeed, as discussed above, the PMF analysis indicates that soil contributes more significantly to particulate absorption in the aged snow samples than in the newly fallen snow samples (Figure 5). A second process that could lead to increases in both C_{BC}^{equiv} and $Å_{tot}$ is melting. Dust particles are generally larger than combustion-sourced particles, and it is expected that the larger particles will be washed down through the snowpack with meltwater less readily than smaller particles [e.g., *Conway et al.*, 1996; *Doherty et al.*, 2013]. Preferential removal of combustion particles (generally, $Å < 2.5$) over dust/soil particles (for these locations, $Å > 3.5$) will simultaneously amplify surface snow mixing ratios and increase $Å_{tot}$.

We thus attribute increases in C_{BC}^{equiv} that are accompanied by increases in $Å_{tot}$ —i.e., all samples with $Å_{tot} > 2.6$ in Figure 4—to a combination of dry deposition of particles with a high soil fraction, followed by possible preferential melt scavenging of lower $Å$ (e.g., combustion) particles versus higher-$Å$ (e.g. soil) particles. Examining Figure 4, we see that C_{BC}^{equiv} exponentially increases from a range of about 60–200 ng g^{-1} to a range of 300–1500 ng g^{-1} as $Å_{tot}$ increases from 2.6 to 4.3. Thus, these processes account for roughly an order of magnitude increase in C_{BC}^{equiv}.

Table 2. Vertical Variations in Newly Fallen Snow at the McCall-A Site, Expressed as the Ratio of C_{BC}^{equiv} and $C_{BC}^{est'}$ in Each Layer to Their Averages Over All Layers[a]

Date	Sample Depth (cm)	Ratio Relative to All Samples on This Day: C_{BC}^{equiv}	$C_{BC}^{est'}$	$Å_{tot}$
29 Jan	0–3	1.47	1.46	1.74
	3–6	0.89	0.94	1.73
	6–9	0.50	0.65	1.64
	9–12	0.58	0.68	1.93
	12–15	1.56	1.27	2.31
4 Feb	0–3	0.55	0.56	1.72
	3–6	0.92	0.93	1.75
	6–9	1.54	1.51	1.51
10 Feb	0–3	1.75	1.25	1.81
	3–6	0.43	0.43	2.05
	6–10	0.82	1.32	1.72
22 Feb	0–2	1.01	1.16	1.63
	2–4	1.18	1.01	1.82
	4–7	0.67	0.75	2.05
	7–10	1.14	1.09	2.09

[a]Also shown are vertical variations in $Å_{tot}$.

3.4. Idaho: Variations Within a New Snowfall Event

At the McCall-A site there were 4 days when 9–15 cm of new snow fell in continuous snowfall events. By sampling the new snow at multiple vertical levels we can study how snow particulate mixing ratios and $Å_{tot}$ varied with time across this single snowfall event. In a simplistic conceptual model where the precipitating cloud and the air mass between cloud level and the ground are advected together one would expect that snowfall would become cleaner with time, as the snow scavenges particles from atmosphere both through ice nuclei activation and the scavenging of aerosols by falling precipitation. We found that while C_{BC}^{equiv} and $C_{BC}^{est'}$ vary significantly within a given snowfall (Table 2), there is no systematic tendency for the snowfall to become cleaner over time (in our samples, towards the top of the snowpack). As in the overall data set, variations in C_{BC}^{equiv} are not correlated with variations in $Å_{tot}$. The lack of a systematic tendency toward cleaner (or dirtier) snow across a single snowfall event likely reflects the complex set of factors that affect the ratio of deposited snow water to particulate mass. For this mountain valley site the source of the upper air mass (where clouds and precipitation form) may be relatively decoupled from the near-surface air (where falling snowflakes gather particles by impaction). Local sources of BC may also have been adding BC to the near-surface air, effectively replenishing the supply of BC available for scavenging.

3.5. Idaho: Spatial Variations in Aged Snow

In previous studies we have shown that the 1 sigma variability in particulate mixing ratios at the 1 m scale is typically 30%, and variability in $Å_{tot}$ is typically 15% [*Doherty et al.*, 2010, 2014; *Wang et al.*, 2013]. Using the sample pairs collected for each site, date, and sample depth, we again found that the absolute differences between sample pairs at the Idaho sites were, on average, 30% (±20%) for C_{BC}^{equiv} and $C_{BC}^{est'}$, but for $Å_{tot}$ the differences were smaller than in our previous study: 5% (±4%).

In addition to quantifying variability at 1 m scale we did a single test of spatial variability at the 10 m scale at the McCall-A site. On the first day of sampling, six randomly distributed profiles, separated by approximately 10 m, were collected. Samples were gathered at the same vertical intervals for all six profiles: of the crust (0–3 cm depth) and of two subsurface layers (3–5.5 cm and 5.5–8.5 cm depth) (Table 3). We calculated the coefficient of variation for each parameter (C_{BC}^{equiv}, $C_{BC}^{est'}$, and $Å_{tot}$) and for each sample layer across all six profiles. We also calculated the absolute value of the fractional difference between each parameter in a given sample layer and the average of that parameter across all samples, i.e., the fractional absolute differences. This quantity is most directly comparable to the average absolute fractional differences between side-by-side pairs reported above. Averaged across all three layers, the absolute fractional differences are quite similar to that of the side-by-side pairs: 30%, 26%, and 6% for C_{BC}^{equiv}, $C_{BC}^{est'}$, and $Å_{tot}$.

Variability across the six profiles for the middle sample layer is comparable to the 1 m scale variability, but it is much lower for the surface layer and much higher for the bottom layer (Table 3). McCall-A is on the frozen Payette Lake, so the deepest layer (5.5–8.5 cm) is sitting on lake ice. As on all sampling days, we tried to sample the bottommost snow without scraping the ice surface, but this layer may contain particles from the ice surface in some profiles, contributing to spatial variability. The surface layer of snow had been exposed to the air—and therefore dry deposition and sublimation—for more than 2 weeks before sampling. It is unclear why this would make the surface snow mixing ratios more spatially uniform.

Table 3. Spatial Variations in C_{BC}^{equiv}, $C_{BC}^{est'}$, and $Å_{tot}$ for Six Vertical Snow Profiles of Approximately 10 m Separation at McCall-A on 27 January 2014[a]

		Profile #							
Sample Depth (cm)	Parameter	1	2	3	4	5	6	Coefficient of Variation	Average Absolute Fraction Difference
0–3	C_{BC}^{equiv}	40.3	47.4	51.0	45.3	40.3	43.9	9%	7%
	$C_{BC}^{est'}$	12.8	10.8	10.2	9.5	9.8	9.8	12%	8%
	$Å_{tot}$	1.26	1.17	1.14	1.15	1.19	1.20	4%	3%
3–5.5	C_{BC}^{equiv}	9.1	6.9	8.3	4.2	6.6	6.7	24%	17%
	$C_{BC}^{est'}$	4.5	3.1	3.5	1.7	2.9	2.9	29%	19%
	$Å_{tot}$	1.83	2.01	1.85	2.26	1.93	1.92	8%	6%
5.5–8.5	C_{BC}^{equiv}	108.5	23.2	16.5	15.3	41.3	18.8	97%	67%
	$C_{BC}^{est'}$	9.1	7.0	5.7	5.9	9.9	6.4	24%	20%
	$Å_{tot}$	2.95	2.21	2.19	2.11	2.10	2.03	15%	10%

[a]The entire snowpack was aged snow; the most recent snowfall was on 11 January. The top layer (0–3 cm) was somewhat crusty, and the middle and bottom layers were pack snow, but snow density in all three layers was similar (180, 200, and 210 kg m^{-3} top to bottom layers, respectively). Shown is the coefficient of variation across all six profiles, as well as the average of the fractional difference, i.e., the absolute difference between one profile's sample and the average across all six profiles.

3.6. Results From Utah

Time series of C_{BC}^{equiv}, $C_{BC}^{est'}$, and $Å_{tot}$ for surface snow at the Vernal, Utah site are plotted in Figure 6. Note that site 16 of D14 was in this same area, as shown in Figures S1 and S3; it was sampled on day 38 of 2013 and included a 0–2 cm deep sample layer, which we can compare to the 0–2.5 cm depth sample on day 38 during the Vernal campaign. After applying the loading-based correction to C_{BC}^{est} from D14 sample we find $C_{BC}^{est'}$ for the two agree to within the 30% small-scale sample variability noted earlier: 15 ng g^{-1} for the D14 sample compared to 17 ng g^{-1} for the Vernal campaign sample. However, C_{BC}^{equiv} is a full 30% higher in the D14 sample (55 ng g^{-1} versus 41.0 ng g^{-1}). For both samples $Å_{tot}$ was 3.1.

In 2013, the start of field measurements coincided with 2 days of new snowfall (indicated by blue stars along the top of the panels in Figure 6), followed by 10 days of no precipitation. $Å_{tot}$ was low in this new snowfall (1.4–1.8). BC mixing ratios ($C_{BC}^{est'}$) in five samples of this new snow vary from 5 to 10 ng g^{-1} and C_{BC}^{equiv} from 12 to 17 ng g^{-1}. Over the next 3 days (DOY 30–32) these mixing ratios increase by just under a factor of three with no new precipitation (Figure 6), likely due to a combination of dry deposition and possibly some melt on DOY 31. Mixing ratios do not increase further until DOY 38–39, when both increase by another factor of 2. Temperatures warmed briefly to above freezing on DOY 37, and this may have driven the observed increase in surface snow mixing ratios on DOY 38 and 39. These increases in C_{BC}^{equiv} and $C_{BC}^{est'}$ are not accompanied by significant changes in $Å_{tot}$, which remains low (1.3–1.7), so if melt did contribute to increased concentrations, there apparently was not preferential washout of BC-rich particles with the melt. This low value of $Å_{tot}$ is consistent with fossil fuel sources; it is much lower than $Å$ of the local soil (4.6).

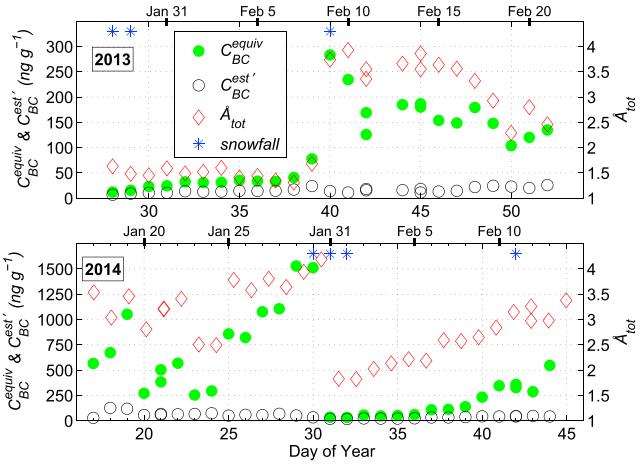

Figure 6. Time series of C_{BC}^{equiv}, $C_{BC}^{est'}$ (left axis), and $Å_{tot}$ (right axis) for the surface samples from the site south of Vernal, Utah in 2013 and 2014. Also shown as blue stars in squares along the top of the plot are days when the surface sample was of newly fallen snow. Surface snow samples varied from 2.5 cm to 5.0 cm in depth.

On DOY 40 (9 February) new snow fell, and this snow was both dirtier (C_{BC}^{equiv} = 283 ng g^{-1}) and browner ($Å_{tot}$ = 3.8) than the existing surface snow, and it contained less BC ($C_{BC}^{est'}$ of 14 ng g^{-1} versus 24 ng g^{-1}). Based on the high value of $Å_{tot}$, we surmise that there is a

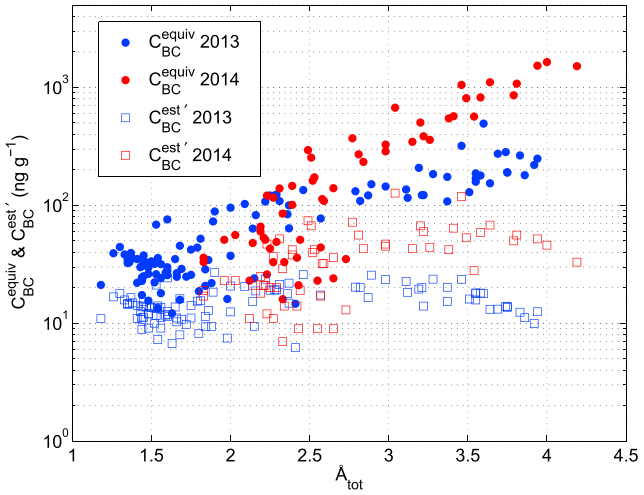

Figure 7. Scatterplot of C_{BC}^{equiv} (dots) and $C_{BC}^{est'}$ (squares) versus $Å_{tot}$ for all samples from the Vernal, Utah site in 2013 (blue) and 2014 (red).

significant amount of dust in these samples. Winds were also somewhat elevated on day 40, consistent with lofting of dust, though it is not clear whether the source of dust in the new snowfall was local. Both C_{BC}^{equiv} and $C_{BC}^{est'}$ in the surface snow decline on days 41–42 relative to the new snow on DOY 40, but this is likely due to the new snow compacting, so the 2.5–5 cm deep surface samples from these days include both the new snow and the cleaner, older snow. After this, C_{BC}^{equiv} varies but has no significant trend. The approximately factor of 2 variability in C_{BC}^{equiv} DOY 44–52 may in part be due to spatial variability, as samples were collected from different locations each day (Figure S3). The mixing ratio of BC in snow over this same period increases from approximately 10–20 ng g^{-1} on DOY 41–47 to 20–25 ng g^{-1} on DOY 48–52, as $Å_{tot}$ decreases from 3.4–3.9 to 2.3–3.3. If surface melt were responsible for this increase, we would expect both C_{BC}^{equiv} and $C_{BC}^{est'}$ to increase. Since only $C_{BC}^{est'}$ increases significantly, we conclude that during this period, there was significant dry deposition of aerosols rich in BC.

The time series in 2014 is nearly the opposite of that in 2013: Initially, high and variable C_{BC}^{equiv} (711 ± 380 ng g^{-1}), $C_{BC}^{est'}$ (68 ± 26 ng g^{-1}), and $Å_{tot}$ (3.3 ± 0.5) for DOY 17–29 all decrease dramatically with new snowfall on DOY 30–32. For DOY 16–27 winds were relatively calm and temperatures only briefly rose above freezing on some days. On DOY 28, high winds may have added to the snowpack local dust from areas in the region lacking snow cover, elevating C_{BC}^{equiv} and $Å_{tot}$ in the samples gathered on DOY 29. On DOY 30, the new snow was quite dirty (C_{BC}^{equiv} = 1500 ng g^{-1}) and brown ($Å_{tot}$ = 4.2), but BC mixing ratios actually declined ($C_{BC}^{est'}$ = 33 ng g^{-1}), consistent with the addition of snow containing significant amounts of dust of $Å_{tot} > 4$ but not much BC. The DOY 30 surface sample may be a mix of new snowfall and the old surface snow. On DOY 31 and 32 samples of new snow are much cleaner and the particles even grayer: C_{BC}^{equiv} = 35 ng g^{-1}, $C_{BC}^{est'}$ = 18 ng g^{-1} and $Å_{tot}$ = 1.9. Winds on these days were calm. After this, all three variables increase nearly linearly from DOY 32 to DOY 41. This is consistent with the steady dry deposition of higher $Å_{tot}$ (i.e., browner) particles than in the DOY 31–32 snowfall, but it is also consistent with surface melt preferentially scavenging lower $Å_{tot}$ (i.e., grayer) particles from the surface snow while simultaneously enhancing surface snow mixing ratios overall. This period coincides with intermittently higher winds and, from DOY 39 onward, with daily average temperatures at or above freezing. Particulate mixing ratios and $Å_{tot}$ in the new snow on DOY 42 are very similar to that in the aged surface snow. On DOY 44 (the last day of the campaign and two days after the new snowfall) C_{BC}^{equiv}, $C_{BC}^{est'}$, and $Å_{tot}$ again have started to increase, accompanied by warming and higher winds.

At the Idaho sites we found that for $Å_{tot} < 2.6$ the variations in C_{BC}^{equiv} were not correlated with $Å_{tot}$ but for $Å_{tot} > 2.6$ C_{BC}^{equiv} increased exponentially with $Å_{tot}$ (Figure 4). At the Utah site the correlation between C_{BC}^{equiv} and $Å_{tot}$ is apparent starting at even lower $Å_{tot}$, especially in 2014 (Figure 7). While measurements of the absorption Ångström exponent of combustion aerosols are somewhat limited and give varying results, $Å_{tot}$ for fossil fuel and biomass burning is generally less than 3, and $Å_{tot}$ is usually lower for fossil fuel combustion aerosol than for biomass burning aerosol due to the lower organic content, though this is not categorically the case. In contrast, the absorption Ångström exponent of the soil from the sites in Idaho is 3.6–5.2 and for Vernal soil is 4.6 (as measured with the ISSW; see supporting information). Thus, increases in $Å_{tot}$ can be indicative of increases in the fraction of particulate light absorption due to soil versus combustion-sourced particles. At the Idaho sites, this hypothesis is supported by the PMF finding of a soil source in aged snow samples. At the

Utah site, the ubiquity of dust in the region provides anecdotal support. It appears likely that at this site light-absorbing particles in snow are a mix of combustion aerosol of low $Å_{tot}$ (i.e., likely fossil fuel aerosol) and dust and that large increases in total particulate light absorption in snow are dominated by deposition of dust.

4. Conclusions

We have presented a study of the evolution of light-absorbing particles in snow from winter to early spring at three sites in the mountains of central Idaho and at one site south of Vernal, Utah. This study provides insights to the magnitude and sources of variability in snow particulate light absorption at these U.S. midlatitude sites, with implications for optimizing both field measurements and modeling of snow particulate mixing ratios and consequent albedo reduction.

This study adds to the growing evidence that dust and soil are often present in snow in sufficient quantities that they compete with or dominate over absorption by BC in snow even at midlatitude sites far from deserts. In earlier studies, desert dust was shown to be the dominant source of light-absorbing particles in seasonal snow in western China [*Wang et al*., 2013; *Zhang et al*., 2013], the Himalaya [*Painter et al*., 2012a], and in the Colorado river basin, where dust in snow has been shown to have both significant radiative forcing and impacts on snowmelt timing and rates [*Painter et al*., 2007, 2010, 2012a, 2012b; *Skiles et al*., 2012, 2015; *Bryant et al*., 2013; *Deems et al*., 2013; *Livneh et al*., 2015]. Soil is also a significant, and sometimes dominant, source of light-absorbing particles in snow in north central China [*Wang et al*., 2013; *Zhang et al*., 2013], central North America [*Doherty et al*., 2014], Utah's Wasatch mountains [*Reyonds et al*., 2014], the California Sierra Nevada mountains [*Sterle et al*., 2013], and the Olympic Peninsula in the northwest corner of Washington State [*Kaspari et al*., 2015]. The dominance of dust in western China and the Colorado Basin and in the Wasatch and Sierra Nevada mountains is not surprising given the proximity to deserts. However, the large role of soil in north central North America and the northwest corner of the continental United States is somewhat more surprising given the lack of nearby deserts. In northwest Washington State the dust was linked to the mobilization of soil following an intense wildfire season [*Kaspari et al*., 2015]. In the north central North America survey of *Doherty et al*. [2014] soil in the snow results from a combination of thin/patchy snow, high winds, and agricultural activity.

For this study, two of the Idaho sites—both mountain valleys in central Idaho—and the site south of Vernal, Utah were also significantly influenced by soil and dust. It is not surprising that desert dust affects the Utah snow, given the arid environment both locally and regionally. *Reyonds et al*. [2014] sourced dust in snow of the Wasatch Mountains of Utah (approximately 200 km west of Vernal) to a region about 225 km southwest of their study region and found that the dust was mixed with urban and industrial components, likely from mining and smelting. In contrast to our Utah site, the significant contribution of local soil to the Idaho snowpacks at both the Cascade Valley and Garden Valley sites was not expected. This source of light-absorbing particles to snow is very likely not accounted for in global and regional models, which generally only account for combustion sources and dust from desert regions.

This study again highlights how critical it is that all sources of particulate light absorption in snow, not just BC, be quantified for a given site, even far from sources of desert dust. Separating the contributions of different absorbers to snow albedo reduction is not straightforward and requires application of multiple techniques. While the SP2 provides perhaps the most direct measure of BC, particulate sampling efficiency may be reduced when the BC is mixed with large quantities of dust, and the BC itself may exist in a large enough size range to cause SP2 uncertainties [*Schwarz et al*., 2012, 2013]. As the SP2 can provide information only about BC, separate measurements are needed to quantify absorption by combustion organics, soil organics, and mineral dust. The technique we used here, the ISSW, measures light absorption by particles deposited on a filter. Mixing ratios of BC in snow are estimated from spectrally resolved absorption. An advantage of this technique is that it measures all components that contribute to albedo reduction. A disadvantage is that as with other filter-based absorption-based measures of BC, there are high biases in inferred BC, especially when large quantities of non-BC components are mixed with the BC. Here we have estimated the magnitude of these biases and made adjustments (on average, downscaling by a factor of 2.5) to our estimates of the mixing ratio of BC in snow ($C_{BC}^{est'}$). This should be kept in mind if comparisons are made to C_{BC}^{est} from earlier studies using the ISSW [*Doherty et al*., 2010, 2013, 2014], as those results were not adjusted for this bias.

The results presented here also highlight the large temporal variability in snow mass mixing ratios and composition at a given site. At the site south of Vernal, Utah, there were large variations in the mixing ratio of BC in snow both within a given year and between years. The mass mixing ratio of BC, $C_{BC}^{est'}$, in the snow was usually in the range 5–25 ng g^{-1} in 2013 but in 2014 was 20–80 ng g^{-1}. Total particulate mixing ratios (C_{BC}^{equiv}) varied by an even greater amount: about 10 to 280 ng g^{-1} in 2013 and 10 to >1000 ng g^{-1} in 2014. While chemical data are not available at the Utah site to confirm this, it appears that dust and soil dominate these large variations in snow particulate absorption. Order of magnitude changes in snow particulate absorption, and large changes in absorption Ångström exponent, were seen from one day to the next, associated with new snowfall events. New snowfall events here were observed to lead to both significant increases in surface snow C_{BC}^{equiv} (e.g., the second half of the sampling period in 2013, when new snow contained high mixing ratios of what appears to be dust) or to significant decreases in C_{BC}^{equiv} (e.g., the second half of the sampling period in 2014, when dust-laden snow was covered with snow containing BC but very little dust).

At the Idaho sites mixing ratios of BC ($C_{BC}^{est'}$) in newly fallen snow varied between about 2 and 10 ng g^{-1}, and all light-absorbing particles (C_{BC}^{equiv}) between 3 and 40 ng g^{-1}. However, mixing ratios in the aged snowpack varied over a much larger range: about 2–40 ng g^{-1} for $C_{BC}^{est'}$ and 3–1000 ng g^{-1} for C_{BC}^{equiv}. Further, in contrast to the Vernal site, newly fallen snow almost always had lower mixing ratios than aged snow at a given site. Thus, processes that occur following snowfall events dominate the variations in snow particulate absorption at these sites.

At the Idaho sites, we estimate that variations in C_{BC}^{equiv} over factors of 2.5–3 can be attributed to sublimation of snow water, dry deposition of aerosol that has the same absorption Ångström exponent (i.e., likely the same composition) as the wet-deposited aerosol, and melt scavenging that does not preferentially remove one absorbing component over another. Dry deposition of, in particular, soil, enhancement of surface particulate mixing ratios with melt, and preferential scavenging of combustion particles (versus soil/dust) from the snow with meltwater causes larger increases; they were responsible for approximately an order of magnitude increase in C_{BC}^{equiv}.

In addition to the large temporal variability, we quantified the spatial variability in snow particulate mixing ratios at a range of scales at the Idaho sites. As in earlier studies in the Arctic [*Doherty et al.*, 2010], north China [*Wang et al.*, 2013], and North America [*Doherty et al.*, 2014] we found spatial variability for C_{BC}^{equiv} and $C_{BC}^{est'}$ at the 1 m spatial scale was about 30%. In the earlier studies, $\AA_{tot}$ typically varied about 15% at this scale; here it was less variable (5%). In an additional test, we found comparable levels of variability at the 10 m scale. At the regional scale, we found that mixing ratios of BC and other light-absorbing particles in falling snow were quite similar at all three Idaho sites, which spanned about 75 km distance (roughly north-south) and about 570 m in altitude. However, differences in the effects of dry deposition and in-snow processes lead to order of magnitude higher total particulate absorption (C_{BC}^{equiv}) in aged snow at the two southern sites, versus the higher, more northern site.

At all three Idaho sites, periods of new snowfall alternated with periods of melting—as is common for many midlatitude regions with seasonal snow cover—and this led to significant day-to-day changes in surface snow mixing ratios. This, and the 1 to 2 orders of magnitude changes in the mixing ratios of BC and dust with new snow at the Vernal, Utah site, emphasize the need for sampling over many days or, at a minimum, of the entire snowpack depth at multiple intervals later in winter, in order to be able to determine the representativeness of a given surface sample. In particular, comparisons of modeled and observed surface snow mixing ratios may differ significantly if even a brief period of rainfall or melt has affected the real snowpack but not the model snowpack (or vice versa, for models that account for the effects of melt on surface snow mixing ratios [*Flanner et al.*, 2007, 2009]). Not accounting for this could lead to false conclusions about model accuracy in representing wet and dry deposition rates.

Acknowledgments

The data presented in this paper can be downloaded from http://www.atmos.washington.edu/articles/IdahoUtah2014. The Idaho measurements and all sample analysis were funded by EPA STAR grant RD-82503801. The Utah study was supported in part by the Western Energy Alliance, and by the NOAA Health of the Atmosphere Program and the NOAA Climate Program Office – Atmospheric Composition and Climate Program. Publication was funded in part by the Joint Institute for the Study of the Atmosphere and Ocean (JISAO) under NOAA Cooperative agreement NA10OAR4320148. It is JISAO contribution 2463 and PMEL Contribution 4377. We thank NOAA/ESRL for providing the meteorological data at the Utah field site and the U.S. Dept. of Agriculture Natural Resource Conservation Service for making SNOTEL data available for the state of Idaho. We warmly thank Anne Greer for use of her home as a residence and laboratory during the Idaho field sampling campaign, the two families that allowed us to use their farms as snow sampling sites in Idaho's Cascade and Garden Valleys, and the Ponderosa State Park staff for their assistance with sampling sites in McCall, Idaho. Helpful comments on the manuscript were received from Teppei Yasunari and two anonymous reviewers.

References

Ahmadov, R., et al. (2015), Understanding high wintertime ozone pollution events in an oil and natural gas producing region of the western US, *Atmos. Chem. Phys.*, *15*, 411–429, doi:10.5194/acp-15-411-2015.

Bond, T. C., T. L. Anderson, and D. Campbell (1999), Calibration and intercomparison of filter-based measurements of visible light absorption by aerosols, *Aerosol Sci. Technol.*, *30*, 582–600.

Bryant, A. C., T. H. Painter, J. S. Deems, and S. M. Bender (2013), Impact of dust radiative forcing in snow on accuracy of operational runoff prediction in the Upper Colorado River Basin, *Geophys. Res. Lett.*, *40*, 3,945–3,949, doi:10.1002/grl.50773.

Conway, H., A. Gades, and C. F. Raymond (1996), Albedo of dirty snow during conditions of melt, *Water Resour. Res.*, *32*(6), 1713–1718, doi:10.1029/96WR00712.
Deems, J. S., T. H. Painter, J. J. Barsugli, J. Belnap, and B. Udall (2013), Combined impacts of current and future dust deposition and regional warming on Colorado River Basin snow dynamics and hydrology, *Hydrol. Earth Syst. Sci.*, *17*(11), 4,401–4,413, doi:10.5194/hess-17-4401-2013.
Doherty, S. J., S. G. Warren, T. C. Grenfell, A. D. Clarke, and R. E. Brandt (2010), Light absorbing impurities in Arctic snow, *Atmos. Chem. Phys.*, *10*, 11,647–11,680, doi:10.5294/acp-10-11647-2010.
Doherty, S. J., T. C. Grenfell, S. Forsström, D. L. Hegg, S. G. Warren, and R. Brandt (2013), Observed vertical redistribution of black carbon and other light-absorbing particles in melting snow, *J. Geophys. Res. Atmos.*, *118*, 5553–5569, doi:10.1002/jgrd.50235.
Doherty, S. J., C. Dang, D. A. Hegg, R. Zhang, and S. G. Warren (2014), Black carbon and other light-absorbing particles in snow of central North America, *J. Geophys. Res. Atmos.*, *119*, 12,807–12,831, doi:10.1002/2014JD022350.
Flanner, M. G., C. S. Zender, J. T. Randerson, and P. J. Rasch (2007), Present-day climate forcing and response from black carbon in snow, *J. Geophys. Res.*, *112*, D11202, doi:10.1029/2006JD008003.
Flanner, M. G., C. S. Zender, P. G. Hess, N. M. Mahowald, T. H. Painter, V. Ramanathan, and P. J. Rasch (2009), Springtime warming and reduced snow cover from carbonaceous particles, *Atmos. Chem. Phys.*, *9*, 2481–2497, doi:10.5194/acp-92481-2009.
Grenfell, T. C., S. J. Doherty, A. D. Clarke, and S. G. Warren (2011), Spectrophotometric determination of absorptive impurities in snow, *Appl. Opt.*, *50*(14), 2037–2048.
Hegg, D. A., S. G. Warren, T. C. Grenfell, S. J. Doherty, T. V. Larson, and A. D. Clarke (2009), Source attribution of black carbon in snow, *Environ. Sci. Technol.*, *43*(11), 4016–4021, doi:10.1021/es803623f.
Hegg, D. A., S. G. Warren, T. C. Grenfell, S. J. Doherty, and A. D. Clarke (2010), Sources of light absorbing aerosol in arctic snow and their seasonal variability, *Atmos. Chem. Phys.*, *10*, 10,923–10,938, doi:10.5194/acp-10-10923-2010.
Judson, A., and N. Doesken (2000), Density of freshly fallen snow in the central Rocky Mountains, *Bull. Am. Meteorol. Soc.*, *81*, 1577–1587.
Kaspari, S., S. M. Skiles, I. Delaney, D. Dixon, and T. H. Painter (2015), Accelerated glacier melt on Snow Dome, Mount Olympus, Washington, USA, due to deposition of black carbon and mineral dust from wildfire, *J. Geophys. Res. Atmos.*, *120*, 2793–2807, doi:10.1002/2014JD022676.
Lack, D. A., C. D. Cappa, D. S. Covert, T. Baynard, P. Massoli, B. Sierau, T. S. Bates, P. K. Quinn, E. R. Lovejoy, and A. R. Ravishankara (2008), Bias in filter-based aerosol light absorption measurements due to organic aerosol loading: Evidence from ambient measurements, *Aerosol Sci. Technol.*, *42*, 1033–1041, doi:10.1080/02786820802389277.
Livneh, B., J. S. Deems, B. Buma, J. J. Barsugli, D. Schneider, N. P. Molotch, K. Wolter, and C. A. Wessman (2015), Catchment response to bark beetle outbreak and dust-on-snow in the Colorado Rocky Mountains, *J. Hydrol.*, *523*, 196–210, doi:10.1016/j.jhydrol.2015.01.039.
Painter, T. H., A. P. Barrett, C. C. Landry, J. C. Neff, M. P. Cassidy, C. R. Lawrence, K. E. McBride, and G. L. Farmer (2007), Impact of disturbed desert soil on duration of mountain snow cover, *Geophys. Res. Lett.*, *34*, L12502, doi:10.1029/2007GL030284.
Painter, T. H., J. S. Deems, J. Belnap, A. F. Hamlet, C. C. Landry, and B. Udall (2010), Response of Colorado River runoff to dust radiative forcing in snow, *Proc. Natl. Acad. Sci. U.S.A.*, *107*(40), 17,125–17,130.
Painter, T. H., A. C. Bryant, and S. M. Skiles (2012a), Radiative forcing by light absorbing impurities in snow from MODIS surface reflectance data, *Geophys. Res. Lett.*, *39*, L17502, doi:10.1029/2012GL052457.
Painter, T. H., S. M. Skiles, J. S. Deems, A. C. Bryant, and C. C. Landry (2012b), Dust radiative forcing in snow of the Upper Colorado River Basin: 1. A 6 year record of energy balance, radiation and dust concentrations, *Water Resour. Res.*, *24*, W07521, doi:10.1029/2012WR011985.
Reynolds, R. L., et al. (2014), Composition of dust deposited to snow cover in the Wasatch Range (Utah, USA): Controls on radiative properties of snow cover and comparison to some dust-source sediments, *Aeolian Res.*, *15*, 73–90, doi:10.1016/j.aeolia.2013.08.001.
Schwarz, J. P., S. J. Doherty, G. L. Kok, F. Li, S. T. Ruggiero, C. E. Tanner, A. E. Perring, R. S. Gao, and D. W. Fahey (2012), Assessing Single Particle Soot Photometer and Integrating Sphere/Integrating Sandwich Spectrophotometer measurement techniques for quantifying black carbon concentration in snow, *Aerosol Meas. Tech.*, *5*, 2581–2592, doi:10.5194/amt-5-2581-2012.
Schwarz, J. P., R. S. Gao, A. E. Perring, J. R. Spackman, and D. W. Fahey (2013), Black carbon aerosol size in snow, *Sci. Rep.*, *3*, 1356, doi:10.1038/srep0-1356.
Skiles, S. M., T. H. Painter, J. S. Deems, A. C. Bryant, and C. C. Landry (2012), Dust radiative forcing in snow of the Upper Colorado River Basin: 2. Interannual variability in radiative forcing and snowmelt rates, *Water Resour. Res.*, *48*, W07522, doi:10.1029/2012WR011986.
Skiles, S. M., T. H. Painter, J. Belnap, L. Holland, R. L. Reynolds, H. L. Goldstein, and J. Lin (2015), Regional variability in dust-on-snow processes and impacts in the Upper Colorado River Basin, *Hydrol. Process.*, doi:10.1002/hyp.10569.
Sterle, K. M., J. R. McConnell, J. Dozier, R. Edwards, and M. G. Flanner (2013), Retention and radiative forcing of black carbon in eastern Sierra Nevada snow, *Cryosphere*, *7*, 365–374, doi:10.5194/tc-7-365-2013.
Wang, X., S. J. Doherty, and J. Huang (2013), Black carbon and other light-absorbing impurities in snow across Northern China, *J. Geophys. Res. Atmos.*, *118*, 1471–1492, doi:10.1029/2012JD018291.
Washenfelder, R. A., et al. (2015), Biomass burning dominates brown carbon absorption in the rural southeastern United States, *Geophys. Res. Lett.*, *42*, 653–664, doi:10.1002/2014GL062444.
Xu, B., J. Cao, D. R. Joswiak, X. Liu, H. Zhou, and J. He (2012), Post-depositional enrichment of black soot in snow-pack and accelerated melting of Tibetan glaciers, *Environ. Res. Lett.*, *7*, doi:10.1088/1748-9326/7/1/014022.
Zhang, R., D. A. Hegg, J. Huang, and Q. Fu (2013), Source attribution of insoluble light-absorbing particles in seasonal snow across northern China, *Atmos. Chem. Phys.*, *13*, 6091–6099, doi:10.5194/acp-13-6091-2013.

Erratum

In the originally published version of this article, text on several pages was incorrectly typeset. These errors have since been corrected and this version may be considered the authoritative version of record.